

## **Closing Report on NKFIH-K 119493 project entitled**

### **“Crosstalk among pathways for prevention, repair, tolerance and potential signaling of uracil-DNA”**

**Principal Investigator: Beáta G. Vértessy**

**Period: 2016-10-01 - 2021-03-31**

#### **Summary**

Nucleotide metabolism and DNA synthesis are key processes in all cells and are under multiple levels of regulation to ensure faithful storage and transmission of genetic information. The appearance of unusual bases in DNA has been traditionally considered as damage sites, however, in recent years, the potential additional significance of these moieties is also addressed. In this final report, I will summarize the major results in the following sections (a full publication list is also enclosed):

#### **1. Uracil-DNA genomic patterns (major publication: Pálinkás et al, eLife, 2020 9:e60498)**

We have focused on uracil (deoxyuridine) in DNA and developed a new full-genome sequencing method specific for uracil (deoxyuridine) moieties in DNA. We termed this method as U-DNA-Seq. Using U-DNA-Seq, we uncovered genome-wide alterations in uracil pattern upon chemotherapeutic drug treatments in human cancer cell line models derived from HCT116. Together with the U-DNA-Seq sequencing method, we also applied super-resolution microscopy to verify uracil patterns. The microscopy allows in situ detection of uracil-DNA and can be also used in numerous different cellular conditions. We identified drug-treatment specific alterations in genomic uracil patterns that provide novel insights into the mechanism of drug action. We also produced a detailed critical review on uracil-DNA detection methods.

#### **2. Models to study uracil-DNA metabolism (major publications: Pálinkás et al, Biomolecules, 2019, 9(4):136, title page adaptation and Rácz et al, 2021, Scientific Reports 11(1):19459)**

Two major pathways are involved in preventing uracil accumulation in DNA: dUTPase-driven elimination of the respective dUTP building block and uracil-DNA-glycosylase-driven excision of uracil from DNA. We have established cellular and animal models for perturbation of these pathways and revealed the role of dUTPase in embryonal development in mouse. We have also established a framework for further reliable gene expression studies in human cells.

#### **3. The role of the DNA deaminase APOBEC3B in mutagenesis (collaborative studies: Nikkila et al, British J Cancer, 2017, 117(1):113 and Periyasamy et al, Nucleic Acids Res, 2017, 45(19):11056)**

Using our U-DNA detection methodologies, we have participated in two major international collaborations aimed at deciphering the regulation of APOBEC3B deaminase. We could directly show increased in genomic uracil levels upon APOBEC3B activation in HEK-293 cells.

#### **4. Further studies linked to dUTPase and uracil-DNA glycosylase, major players in uracil-DNA metabolism**

During the running of the NKFIH-K 119493 project, we also continued our structure-function studies on dUTPases, related pyrophosphatases and uracil-DNS glycosylases. These studies are related to this project, but do not fall within its major focus, hence I will only shortly list the articles generated from these studies (support of this project is also acknowledged in these publications).

The funding for this project was acknowledged in 20 international, peer-reviewed publications (see list at the end of this report)

Below, some major results are described, based on the published journal articles, separated into the four sections mentioned above. All details are thoroughly described in our published articles.

With regards to the original Aims and workplan of this project, during the research we decided to focus on the most significant studies and modified our research strategy, accordingly. Namely, successful application in our models to gain uracil-DNA patterns required regrouping our efforts. This strategy led to an eLife publication and other major papers. Nanopore sequencing trials did not produce reliable patterns. With the current technological developments, we now plan to again try this approach for uracil-DNA sequencing, however, this will be a future project. The uracil-mapping workload did not allow us to finish and publish the planned experiments for the *Drosophila* studies.

## 1. Uracil-DNA genomic patterns

Among the non-canonical bases in DNA, uracil can occur either through cytosine deamination or thymine-replacing incorporation. Both the immediate cause and consequence of these two routes are different, as shown on Figure 1. No matter how uracil gets into DNA, cells act against this incorporation by activating uracil-excision repair, where the first reaction is cleavage of the uracil base from the DNA catalyzed by the uracil-DNA glycosylase (UDG) enzymatic activity.

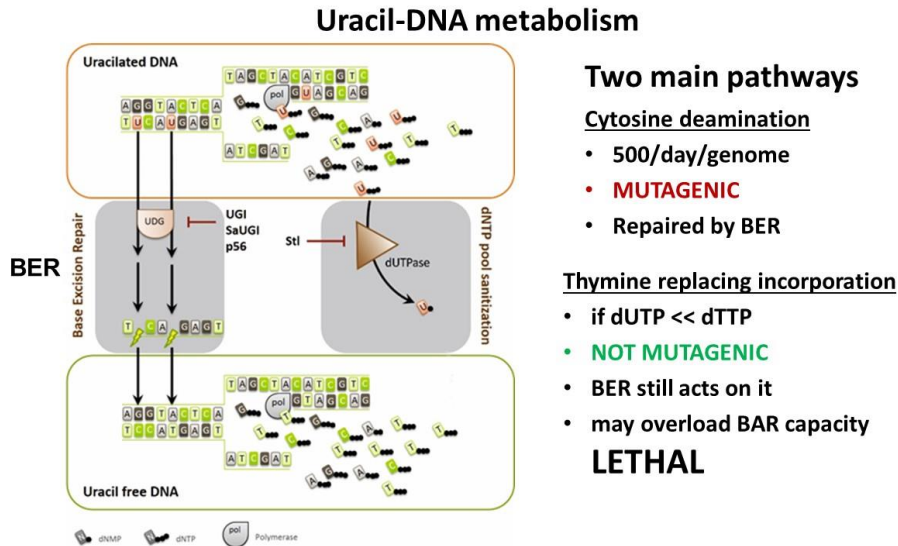


Figure 1. Uracil-DNA metabolism. The two pathways for uracil incorporation into DNA are shown, together with the action of dUTPase to sanitize the dNTP pool by cleaving dUTP and the uracil-excision catalyzed by UDG. Proteinaceous inhibitors against dUTPase (Stl) and against UDG (UGI, SaUGI and p56) are also indicated.

Uracil is among the most frequently occurring mistakes in human DNA mostly due to the inherent aerobic environment that facilitates cytosine deamination. It has been estimated that a human-sized genome suffers about 500 cytosine deamination events, leading to a mutagenic process. Also, nucleotide pool perturbations, namely increase in dUTP levels, leads to uracil (dUMP) incorporation as thymine replacements. This latter route is not mutagenic, *per se*, and is quite sufficiently inhibited due to the enzymatic action of dUTPase. The product of the dUTPase catalytic reaction is dUMP that is also the substrate for thymidylate synthase. Therefore dUTPase action has a dual role - removal of dUTP and supply of dUMP – both of which contributes to a low dUTP/dTTP ratio. Uracil excision through base-excision repair (BER) is a highly efficient process and does not distinguish cytosine deaminated or thymine replacing uracils. During BER, the uracil base is cut out and the abasic site is further processed by endonuclease leading to a DNA strand break. The final events of BER require repair synthesis, and under high dUTP levels the repair will re-introduce uracil against adenine. Therefore, high dUTP levels initiate a hyperactive

futile cycle of uracil-excision repair and this finally culminates in DNA fragmentation and cell death. Numerous anticancer drugs (such as 5-fluorouracil (5-FU), 5-fluoro-2'-deoxyuridine (5FdUR), capecitabine, methotrexate, raltitrexed (RTX), pemetrexed) targeting thymidylate biosynthesis act upon this rationale: these lead to an increase in the dUTP/dTTP ratio thereby inducing DNA uracilation with the ultimate result of genome fragmentation and cell death preferentially in the fast-dividing cancer cells.

DNA uracilation is therefore of high biomedical significance in anticancer therapy. Also, several physiological circumstances in e.g. antibody maturation require uracil in DNA. It is therefore of high interest to investigate uracil distribution patterns in DNA. Usual sequencing methods are, however, transparent to uracil (as to all non-canonical DNA bases), necessitating the development of focused approaches. Before starting our project, no such method was described in the literature, necessitating our research in this important issue. We planned our uracil-DNA sequencing method (U-DNA-Seq) based on an uracil-sensor previously developed in our lab. This sensor contains the uracil-recognizing domain of the human UNG enzyme but it is catalytically inactive due to two mutations we have introduced in the active site. The uracil-binding capability of mutant UNG is still preserved. Using a tagged version of this uracil-sensor (FLAG-tagged catalytically inactive  $\Delta$ UNG sensor), we have applied a pull-down procedure (shown below on Figure 2, panel A).

It follows from the above-described pathways that uracil presence in cellular DNA is transient if uracil-DNA glycosylase (UDG) activity is present. UDG activity is supplied by numerous isoforms in human cells, in line with the important requirement for the repair of uracils. The elusive short-lived presence of genomic uracils prevents their in-depth characterization and in order to track nascent uracils, we developed HCT116 cell lines where the most efficient UDG isoform (UNG) is counteracted by its formidable inhibitor, UGI (uracil-DNA glycosylase inhibitor protein). We chose a human colon carcinoma cell line, HCT116 and its mismatch repair (MMR) proficient variant as well-established and relevant cellular models. We created cell lines either transiently or stably expressing UGI (stable expression was achieved through retroviral-based insertion of UGI on the cell chromosome). In these cells, we could observe the otherwise transient genomic uracils, as shown on Figure 2. We performed immunoprecipitation by applying the FLAG-tagged catalytically inactive  $\Delta$ UNG sensor to bind to uracil in purified and fragmented genomic DNA, followed by a pull-down with anti-FLAG agarose beads. We proceeded to treat the UGI-expressing cells with either 5FdUR or RTX, two drugs widely used in anticancer chemotherapy that act by perturbing thymidylate biosynthesis since these drugs inhibit the thymidylate synthase enzyme. We showed that combination of UGI expression and drug treatment led to significant increase in genomic uracil levels (Figure 2, panel B and Figure 3). We also found that the uracil-DNA levels are increased when the MMR status is restored to the HCT116 cells (Figure 3).

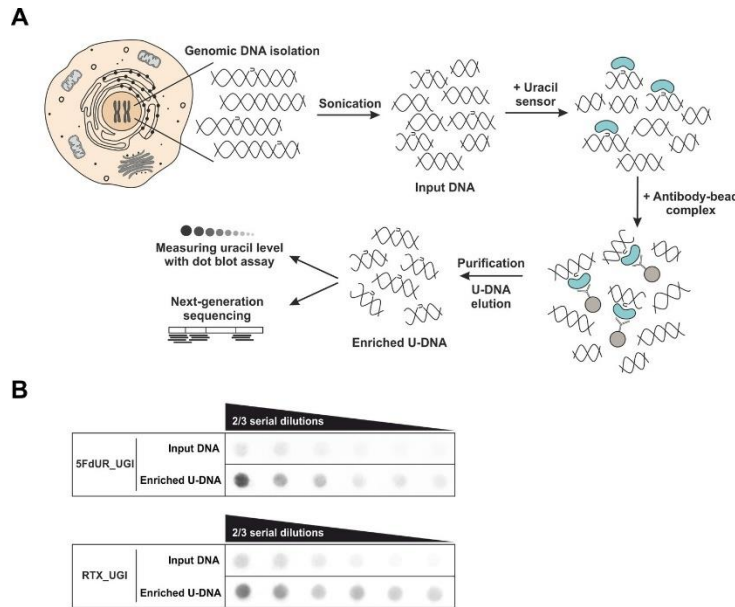


**Figure 2. Scheme and application of the uracil-sensor** (taken from our article Pálinkás HL, et el, Vértessy BG. entitled” Genome-wide alterations of uracil distribution patterns in human DNA upon chemotherapeutic treatments.” *Elife*. 2020 Sep 21;9:e60498.) (A) Schematic image of the novel U-DNA immunoprecipitation and sequencing method (U-DNA-Seq). After sonication, enrichment of the fragmented U-DNA was carried out by the 1xFLAG-ΔUNG sensor construct followed by pull-down with anti-FLAG agarose beads. U-DNA enrichment compared to input DNA was confirmed by dot blot assay before samples were subjected to next generation sequencing. (B) Immunoprecipitation led to elevated uracil levels in enriched U-DNA samples compared to input DNA in case of both 5FdUR (5FdUR\_UGI) and RTX (RTX\_UGI) treated, UGI-expressing HCT116 samples.

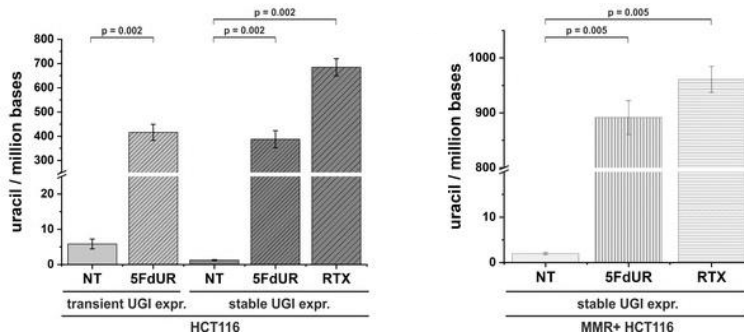


**Figure 3. Increase in genomic uracil levels upon drug treatment in UGI-expressing HCT116 cells** (taken from our article Pálinkás HL, et el, Vértessy BG. *Elife*. 2020 Sep 21;9:e60498.) Drug treatment led to significantly elevated uracil levels, also depending on the absence or presence of the MMR apparatus in the cells.

Next, we proceeded to determine genome-wide distribution of uracils upon drug treatment in both MMR-deficient and MMR-proficient cells. Our paper in eLife details these findings, here in the final report, I wish to emphasize the major conclusions. First of all, to correctly interpret the sequencing data avoiding false technical errors, we had to develop a novel bioinformatic pipeline taking into account that U-DNA-Seq is not a base-resolution method but generates segment-wide data. With this pipeline we got reproducible data and could analyze genomic uracil patterns generated under different conditions. As shown on Figure 4, uracil-enrichment coverage tracks revealed altered distribution of uracil-containing regions in the drug-treated as compared to the non-treated samples. Also, drug-specific alterations in the uracil-distribution are evident (cf yellow highlights on Figure 4). Especially in the case of 5FdUR-treatment, the MMR status also alters uracil-distribution patterns (cf pink highlights on Figure 4). These changes in U-DNA patterns were confirmed when we checked how uracil-patterns correlate to several histone markers (cf details in the eLife paper).

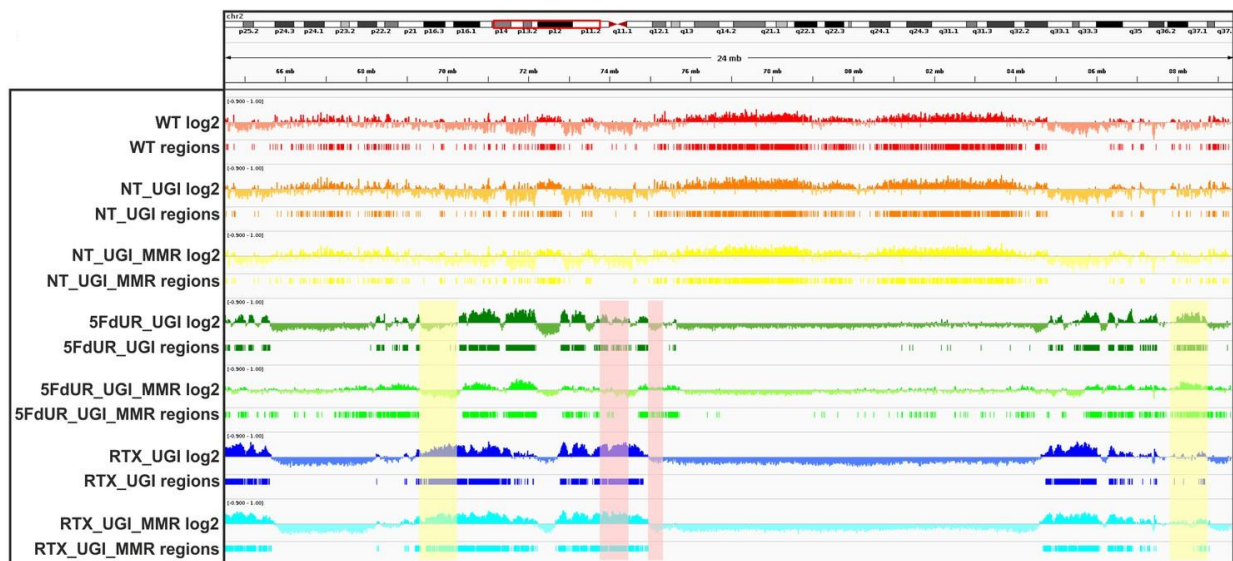
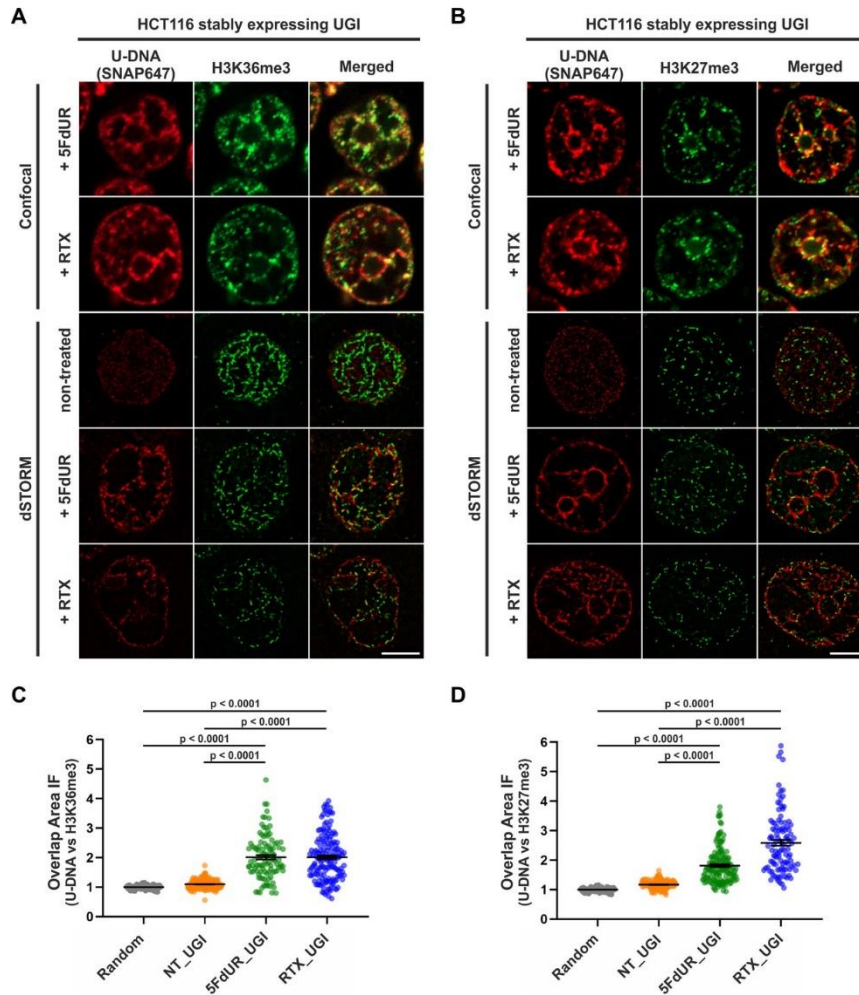


Figure 4. Genomic uracil levels change upon drug treatment and the MMR status (taken from our article Pálinkás HL, et al, Vértessy BG. Elife. 2020 Sep 21;9:e60498.) Figure shows log<sub>2</sub> ratio signal tracks of enriched versus input coverage (log<sub>2</sub>, upper tracks) and derived regions of uracil enrichment (regions, bottom tracks) for non-treated: wild type (WT, red), UGI-expressing (NT\_UGI, orange), and MMR proficient UGI-expressing (NT\_UGI\_MMR, yellow); and for treated: with 5FdUR (5FdUR\_UGI, green; 5FdUR\_UGI\_MMR, light green) or raltitrexed (RTX\_UGI, blue; RTX\_UGI\_MMR, cyan) HCT116 samples. Figure shows patterns in the genomic segment (chr2:64,500,000–89,500,001) – all data are available as supplementary material to our eLife paper.

Another highlight of this study is that uracil-patterns could also be observed and quantitatively analyzed using in situ super-resolution dSTORM microscopy (Figure 5). We could also verify that histone marks colocalization derived from genomic distribution patterns can be seen in the in situ co-staining samples. Hence, the U-DNA-Seq method proved to be a powerful and straightforward approach. Consequently, we have been contacted by numerous laboratories interested in this methodology with the aim to pursue this approach in varied physiological conditions.



**Figure 5. Genomic uracil moieties colocalize with H3K36me3 and H3K27me3 analyzed by super-resolution microscopy.** (taken from our article Pálinkás HL, et al, Vértessy BG. *Elife*. 2020 Sep 21;9:e60498.) Confocal and dSTORM imaging were performed on non-treated, 5FdUR or RTX treated HCT116 cells stably expressing UGI to compare the localization of genomic uracil residues (red) to histone markers, H3K36me3 (green) (A) or H3K27me3 (green) (B). Scale bar represents 5  $\mu$ m. The graphs display the cross-pair correlation analysis between U-DNA and H3K36me3 (C) or H3K27me3 (D) performed on dSTORM images. Overlap is defined as any amount of pixel overlap between segmented objects. Total numbers of analyzed nuclei for H3K36me3 staining (C) were the following: NT\_UGI (n = 205), 5FdUR\_UGI (n = 101) and RTX\_UGI (n = 153) from two independent experiments. Total numbers of analyzed nuclei for H3K27me3 staining (D) were the following: NT\_UGI (n = 154), 5FdUR\_UGI (n = 151) and RTX\_UGI (n = 107) from two independent experiments. Black line denotes the mean of each dataset, and error bars represent standard errors of the mean (SEM).

Based on our studies and deep interest in uracil-DNA, we also wrote a review entitled “Detection of Genomic Uracil Patterns” (publication: Békési A, Holub E, Pálinkás HL, Vértessy BG. *Int J Mol Sci*. 2021 Apr 9;22(8):3902.)

## 2. Models to study uracil-DNA metabolism

We have developed two types of models: cell lines and transgenic mouse. In the cell line models, we have started from the HCT116 cell line (cf also the previous section in this report). This cell line lacks the mismatch repair apparatus (it has a chromosomal defect on chromosome 3 involving the gene for the MLH1 protein that has an important role in MMR). We also used the isogenic cell line where an intact copy of chromosome 3 is added to the genome (HCT116chr3+). In both cell lines we successfully inserted the gene for the UGI protein into the genome for stable transfection, and we also created transiently transfected cells. The expression of the UGI protein in these assays is linked to the expression of the EGFP fluorescent protein. We used retroviral transduction and selected EGFP-positive cells (Figure 6).

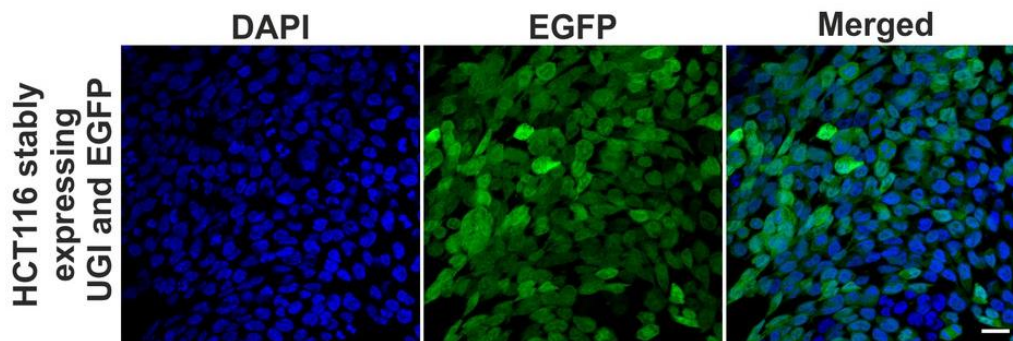
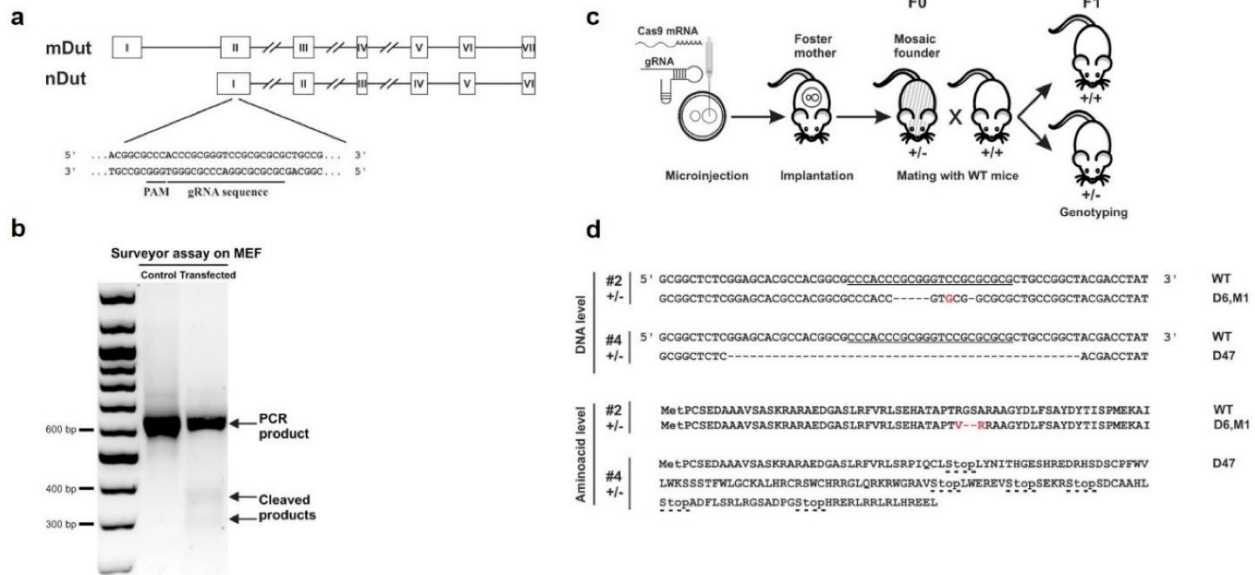


Figure 6. HCT116 cells stably expressing UGI and EGFP (taken from our article Pálinkás HL, et al, Vértessy BG. *Elife*. 2020 Sep 21;9:e60498.) HCT116 cells stably expressing UGI along with EGFP following retroviral transduction. GFP positive cells were selected by fluorescence-activated cell sorting and cultured for further analysis. DAPI was used for DNA staining. Scale bar represents 20  $\mu$ m.

We could successfully create the UGI-expressing cell line also from the HCT116chr3+ - ie MMR proficient cell line, as well.

We have tried Crispr-based generation of transgenic cell lines for knocking out dUTPase, and also pursued ZFN-based genome engineering for conditional dUTPase knock-out. Despite numerous trials, we could not generate dUTPase knock-outs. The exact reason for this failure is not yet fully understood. It may be a direct indication of dUTPase being absolutely essential, however, we still need additional evidence for this. However, we could successfully generate dUTPase knock-out (*dut*<sup>-/-</sup> genotype) in mouse.

For the transgenic mice experiments, we designed the relevant Crispr constructs and developed the *dut*<sup>-/-</sup> genotype mice, in collaboration with Drs László Hiripi and Elen Gócza, as shown in Figure 7 below.



**Figure 7. Generation and assessment of CRISPR knock-out mice.** (taken from our paper Pálinkás et al, 2019, Biomolecules 9(4):136.) (a) Schematic diagram of the *dut* gene encoding the nuclear (nDut) and mitochondrial (mDut) isoforms of deoxyuridine 5'-triphosphate nucleotidohydrolase (dUTPase). Exons are indicated with Roman numerals in rectangles, introns are simplified as lines (for longer introns lines are broken). Guide RNA (gRNA) target site and protospacer-adjacent motif (PAM) sequence in the first common exon of the two isoforms are underlined. (b) Surveyor assay performed on mouse embryonic fibroblast (MEF) cells used for the detection of indel events induced by transfection with CRISPR gRNA and Cas9 mRNA. The two lower fragments indicate cleavage of the DNA due to CRISPR activity. These are lacking in the control while they are visible in the transfected sample. (c) Schematic diagram showing the generation of CRISPR-targeted knock-out mice. Fertilized oocytes microinjected with gRNA and Cas9 mRNA were implanted into foster mothers. The resulting founders (F0) #2 and #4 were cross-bred with wild-type (WT) mice to generate wild-type (*dut* +/+) and heterozygous (*dut* +/-) offspring (F1) containing the targeted locus through germline transmission. (d) DNA and predicted amino acid sequence of the two heterozygous founder mice (#2 and #4) showing CRISPR events, compared to the WT. Mouse #2 showed deletion of six nucleotides and a C to G mutation (D6, M1) resulting in the deletion of two amino acids and change of another two. In mouse #4, 47 nucleotides were deleted (D47) which resulted in a frameshift mutation leading to early stop codons indicated with dashed lines. CRISPR target site including PAM sequence is underlined.

Investigations of embryonal development and live birth events from the heterozygous (*dut* +/-) crossing, we revealed that *dut* -/- embryos could only be observed at early pre-implantation stages. We found that all three genotypes (+/+, +/-, -/-) resulted in live 3.5-day-old embryos. Our results showed that the dUTPase knock-out did not affect the first several duplication cycles and viable blastocysts could be isolated. Furthermore, isolated *dut* -/- blastocysts could grow further in *in vitro* cultures, although outgrowth of both the inner cell mass and the trophectoderm cells were impaired. However, further development following implantation was prevented in the homozygous knock-out embryo.

The article describing these findings was selected as title page illustration, as shown on Figure 8.

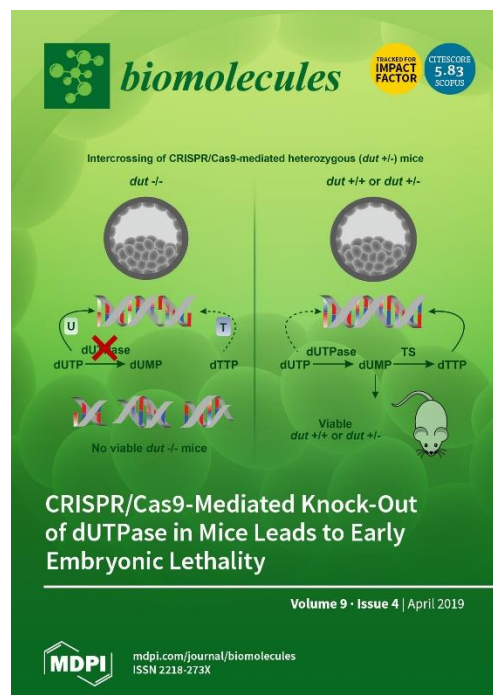


Figure 8. Title page illustration of our article Pálinkás et al., 2019, *Biomolecules* 9(4):136). The impact factor of the journal *Biomolecules* was determined as 3.910, with Q1 Scimago classification in Biochemistry.

Having found that the *dut*<sup>-/-</sup> genotype leads to early embryonic lethality, it was of immediate interest to investigate the mechanism of this lethality. It is known that lack of dUTPase leads to genome fragmentation, and we wished to decide if this may be counteracted by impeding uracil-DNA excision repair. For this, we wanted to decide if the parallel knock-out in uracil-DNA excising glycosylases may rescue the lethal phenotype. In mice, two of the uracil-DNA glycosylases isoforms UNG and SMUG are responsible for the major part of uracil excision events. We therefore crossed the *dut*<sup>+/-</sup> animals with *ung*<sup>-/-</sup>:*smug*<sup>-/-</sup> animals and found that no triple KOs could be identified among the newborns. Also, we discovered that UNG and SMUG KOs had no beneficial effect on the embryonal development of the triple KO embryos. These data are yet unpublished, we are working further to investigate the mechanism of lethality caused by dUTPase knock-out.

During the present project, we also shed light on the dUTPase expression patterns in different mouse tissues towards a better understanding of the physiological role of the enzyme (publication: Racz et al, 2019 *FEBS Open Bio* 9(6):1153-1170). In addition, in order to further investigate dUTPase expression levels in a variety of human cell lines under different circumstances using reliable controls, we established a set of new reference genes with stable expression patterns for gene expression studies (publication: Racz et al, 2021, *Scientific Reports*, 11(1):19459).

### **3. The role of the DNA deaminase APOBEC3B in mutagenesis (collaborative studies)**

Our previous publication on developing a sensitive and well reproducible uracil-DNA quantitative method using a dot-blot approach (publication Rona et al, 2016, *Nucleic Acids Research*, 44:e28) was well received in the scientific community and led to several collaborations. Two of such collaborative studies were completed successfully during the present project and resulted in two collaborative articles.

In one of these, we have investigated the cellular phenotypes associated with high-level APOBEC3B expression and the influence of p53 status on these phenotypes using an isogenic system (publication: Nikkilä J, et al: Elevated APOBEC3B expression drives a kataegic-like mutation signature and replication stress-related therapeutic vulnerabilities in p53-defective cells. *Br J Cancer*. 2017 Jun 27;117(1):113-123). APOBEC3B is a DNA deaminase enzyme that leads to cytosine to uracil deamination, and it was of immediate interest to apply our method for a direct analysis of uracil-DNA levels. We could show that APOBEC3B induction led to the functional consequence of elevation of uracil-DNA levels. We also revealed that although APOBEC3B expression increased the incorporation of genomic uracil, invoked DNA double-strand-break repair biomarkers and caused cell cycle arrest, inactivation of p53 circumvented APOBEC3B-induced cell cycle arrest without reversing the increase in genomic uracil or the double-strand-break repair biomarkers.

In the second collaborative study, we have further investigated the role of p53-dependent regulation of APOBEC3B (publication: Periyasamy et al: p53 controls expression of the DNA deaminase APOBEC3B to limit its potential mutagenic activity in cancer cells. *Nucleic Acids Research*. 2017 Nov 2;45(19):11056-11069). We showed that perturbation of the correct regulatory pattern leads to elevated APOBEC3B expression and cytosine deaminase activity in cancer cells.

### **4. Further studies linked to dUTPase and uracil-DNA glycosylase, major players in uracil-DNA metabolism**

During the present project, we also published several papers to address general issues of uracil-DNA metabolism and structure-function studies of related enzymes. These publications are also listed below. Using our uracil-DNA dot-blot assay, we could detect elevated uracil-DNA levels at several stages of the malaria parasite *Plasmodium falciparum* (publication #8 in the publication list).

We published structure-function studies on dUTPases (publications #9-16), uracil-DNA glycosylase (publications #17) and dUTPase-related pyrophosphatases (CCT enzymes, publications #18-19). We also published a review on therapeutic approaches against pathogenic microorganisms targeting the key players of thymidylate biosynthesis: dUTPases, thymidylate synthases and dihydrofolate reductases (publication #20).

**List of papers published with acknowledgment of OTKA support  
during the present project**

1: Pálinkás HL, Békési A, Róna G, Pongor L, Papp G, Tihanyi G, Holub E, Póti Á, Gemma C, Ali S, Morten MJ, Rothenberg E, Pagano M, Szűts D, Győrffy B, **Vértessy BG.**

Genome-wide alterations of uracil distribution patterns in human DNA upon chemotherapeutic treatments.

Elife. 2020 Sep 21;9:e60498. doi:10.7554/eLife.60498. **D1**

2: Békési A, Holub E, Pálinkás HL, **Vértessy BG.**

Detection of Genomic Uracil Patterns.

Int J Mol Sci. 2021 Apr 9;22(8):3902. doi: 10.3390/ijms22083902. **Q1**

3: Pálinkás HL, Rác Z, Gál Z, Hoffmann OI, Tihanyi G, Róna G, Gócsa E, Hiripi L, **Vértessy BG.**

CRISPR/Cas9-Mediated Knock-Out of dUTPase in Mice Leads to Early Embryonic Lethality.

Biomolecules. 2019 Apr 4;9(4):136. doi:10.3390/biom9040136. **Q1**

4: Rác Z, Nagy N, Gál Z, Pintér T, Hiripi L, **Vértessy BG.**

Evaluation of critical design parameters for RT-qPCR-based analysis of multiple dUTPase isoform genes in mice.

FEBS Open Bio. 2019 Jun;9(6):1153-1170. doi:10.1002/2211-5463.12654. **Q2**

5: Rác Z, Nagy N, Tóvári J, Apáti Á, **Vértessy BG.**

Identification of new reference genes with stable expression patterns for gene expression studies using human cancer and normal cell lines.

Sci Rep. 2021 Sep 30;11(1):19459. doi:10.1038/s41598-021-98869-x. **D1**

6: Nikkilä J, Kumar R, Campbell J, Brandsma I, Pemberton HN, Wallberg F, Nagy K, Scheer I, **Vértessy BG,** Serebrenik AA, Monni V, Harris RS, Pettitt SJ, Ashworth A, Lord CJ.

Elevated APOBEC3B expression drives a kataegic-like mutation signature and replication stress-related therapeutic vulnerabilities in p53-defective cells.

Br J Cancer. 2017 Jun 27;117(1):113-123. doi:10.1038/bjc.2017.133. **D1**

7: Periyasamy M, Singh AK, Gemma C, Kranjec C, Farzan R, Leach DA, Navaratnam N, Pálinkás HL, **Vértessy BG,** Fenton TR, Doorbar J, Fuller-Pace F, Meek DW, Coombes RC, Buluwela L, Ali S.

p53 controls expression of the DNA deaminase APOBEC3B to limit its potential mutagenic activity in cancer cells.

Nucleic Acids Res. 2017 Nov 2;45(19):11056-11069. doi: 10.1093/nar/gkx721. **D1**

8: Molnár P, Marton L, Izrael R, Pálinkás HL, **Vértessy BG**.

Uracil moieties in *Plasmodium falciparum* genomic DNA.

FEBS Open Bio. 2018 Sep 29;8(11):1763-1772. doi: 10.1002/2211-5463.12458. **Q2**

9: Hirmondo R, Lopata A, Suranyi EV, **Vértessy BG**, Toth J.

Differential control of dNTP biosynthesis and genome integrity maintenance by the dUTPase superfamily enzymes.

Sci Rep. 2017 Jul 20;7(1):6043. doi: 10.1038/s41598-017-06206-y. **D1**

10: Nyíri K, Harris MJ, Matejka J, Ozohanics O, Vékey K, Borysik AJ, **Vértessy BG**.

HDX and Native Mass Spectrometry Reveals the Different Structural Basis for Interaction of the Staphylococcal Pathogenicity Island Repressor StI with Dimeric and Trimeric Phage dUTPases.

Biomolecules. 2019 Sep 14;9(9):488. doi:10.3390/biom9090488. **Q1**

11: Benedek A, Pölöskei I, Ozohanics O, Vékey K, **Vértessy BG**.

The StI repressor from *Staphylococcus aureus* is an efficient inhibitor of the eukaryotic fruitfly dUTPase.

FEBS Open Bio. 2017 Dec 27;8(2):158-167. doi:10.1002/2211-5463.12302. **Q2**

12: Nyíri K, Mertens HDT, Tihanyi B, Nagy GN, Kőhegyi B, Matejka J, Harris MJ, Szabó JE, Papp-Kádár V, Németh-Pongrácz V, Ozohanics O, Vékey K, Svergun DI, Borysik AJ, **Vértessy BG**.

Structural model of human dUTPase in complex with a novel proteinaceous inhibitor.

Sci Rep. 2018 Mar 12;8(1):4326. doi:10.1038/s41598-018-22145-8. **D1**

13: Surányi ÉV, Hírmondó R, Nyíri K, Tarjányi S, Kőhegyi B, Tóth J, **Vértessy BG**.

Exploiting a Phage-Bacterium Interaction System as a Molecular Switch to Decipher Macromolecular Interactions in the Living Cell.

Viruses. 2018 Apr 1;10(4):168. doi: 10.3390/v10040168. **Q1**

14: Benedek A, Temesváry-Kis F, Khatanbaatar T, Leveles I, Surányi ÉV, Szabó JE, Wunderlich L, **Vértessy BG**.

The Role of a Key Amino Acid Position in Species-Specific Proteinaceous dUTPase Inhibition.

Biomolecules. 2019 Jun 6;9(6):221. doi: 10.3390/biom9060221. **Q1**

15: Lopata A, Jójárt B, Surányi ÉV, Takács E, Bezúr L, Leveles I, Bendes ÁÁ, Viskolcz B, **Vértessy BG**, Tóth J.

Beyond Chelation: EDTA Tightly Binds Taq DNA Polymerase, MutT and dUTPase and Directly Inhibits dNTPase Activity.

Biomolecules. 2019 Oct 17;9(10):621. doi: 10.3390/biom9100621. **Q1**

16: Nagy GN, Suardiaz R, Lopata A, Ozohanics O, Vékey K, Brooks BR, Leveles I, Tóth J, **Vértessy BG**, Rosta E.

Structural Characterization of Arginine Fingers: Identification of an Arginine Finger for the Pyrophosphatase dUTPases.

J Am Chem Soc. 2016 Nov 16;138(45):15035-15045. doi: 10.1021/jacs.6b09012. **D1**

17: Papp-Kádár V, Balázs Z, Vékey K, Ozohanics O, **Vértessy BG**.

Mass spectrometry-based analysis of macromolecular complexes of *Staphylococcus aureus* uracil-DNA glycosylase and its inhibitor reveals specific variations due to naturally occurring mutations.

FEBS Open Bio. 2019 Feb 9;9(3):420-427. doi: 10.1002/2211-5463.12567. **Q2**

18: Guca E, Nagy GN, Hajdú F, Marton L, Izrael R, Hoh F, Yang Y, Vial H, **Vértessy BG**, Guichou JF, Cerdan R.

Structural determinants of the catalytic mechanism of Plasmodium CCT, a key enzyme of malaria lipid biosynthesis.

Sci Rep. 2018 Jul 25;8(1):11215. doi: 10.1038/s41598-018-29500-9. **D1**

19: Marton L, Hajdú F, Nagy GN, Kucsma N, Szakács G, **Vértessy BG**.

Heterologous expression of CTP:phosphocholine cytidyltransferase from Plasmodium falciparum rescues Chinese Hamster Ovary cells deficient in the Kennedy phosphatidylcholine biosynthesis pathway.

Sci Rep. 2018 Jun 12;8(1):8932. doi:10.1038/s41598-018-27183-w. **D1**

20: Nyíri K, **Vértessy BG**.

Perturbation of genome integrity to fight pathogenic microorganisms.

Biochim Biophys Acta Gen Subj. 2017 Jan;1861(1 Pt B):3593-3612.

doi: 10.1016/j.bbagen.2016.05.024. **Q1**